DATA PAPER

Asymmetry parameters in single ionization of He, Ne by XUV pulses

Jian-Ting Lei(雷建廷)[1,2,†], Xuan Yu(余璇)[1,2,†], Guo-Qiang Shi(史国强)[1], Chen-Yu Tao(陶琛玉)[2,3], Shao-Hua Sun(孙少华)[1], Shun-Cheng Yan(闫顺成)[2,3], Xin-Wen Ma(马新文)[2,3], Jing-Jie Ding(丁晶洁)[1,‡], and Shao-Feng Zhang(张少锋)[2,3,§]

[1] *School of Nuclear Science and Technology, Lanzhou University, Lanzhou* 730000, *China*
[2] *Institute of Modern Physics, Chinese Academy of Sciences, Lanzhou* 730000, *China*
[3] *University of Chinese Academy of Sciences, Beijing* 100049, *China*

(Received 6 October 2022; revised manuscript received 12 November 2022; accepted manuscript online 29 November 2022)

Fully differential cross-sections of single ionization of He and Ne atoms are studied by linearly polarized extreme ultraviolet (XUV) photons in the energy range of 22.1 eV–43.7 eV, using a reaction microscope. Photoelectron angular distributions and the β asymmetry parameters for He $1s^2$ electrons prove the reliability of our experiment, and the β asymmetry parameters extracted from the angular distributions of Ne $2p^6$ electrons are obtained. By comparing with different theoretical calculations, it is found that the contribution of the electron correlation effect in Ne $2p^6$ single ionization becomes increasingly important as the incident photon energy increases, while the relativistic effect is relatively low in the whole incident energy range. Our experimental β asymmetry parameters may serve as a significant reference to test the most elaborated theories in the field. The datasets presented in this paper, including the photoelectron angular distributions and β asymmetry parameters, are openly available at https://doi.org/10.57760/sciencedb.j00113.00073.

Keywords: photoelectron angular distribution, β asymmetry parameter, reaction microscope

PACS: 32.80.–t, 32.10.–f, 42.55.Vc **DOI:** 10.1088/1674-1056/aca6d9

1. Introduction

Photoionization is one of the fundamental processes in nature where detailed information about few-body dynamics can be extracted from single and multiple ionization processes.[1–5] Regarding the closed shells of noble atoms, they are much easier to be handled in experiments and, for the theoretical part, it also dramatically simplifies the models where descriptions of these processes are much easier.[6,7] In spite of such simplification, it is still challenging to get satisfactory descriptions. For instance, in the work of Ref. [8], photoelectron spectra of Ar, Kr, and Xe with the resolution of 0.5 eV were studied where significant discrepancies were found at the spin–orbit splitting levels between experimental data and theoretical predictions. In a later study, satellite line profiles in high-resolution photoelectron energy spectra were systematically studied for He, Ne, Ar, Kr, and Xe. In the regime of ionization threshold, the energy spectra profiles were revealed in the case of the $2s2p^5nl$ satellites of Ne and asymmetric Fano line shapes indicate the strong electron correlations.[9] Parallel to the single ionization, double and multiple ionizations of rare gases have also been studied. In 1967, double and multiple ionizations of He, Ne, and Ar were first observed using monochromatized XUV photon of the energy about 278 eV. In that work, the measured double ionization cross sections were found larger than predictions based on the single electron approximation and it is concluded that electron correlations are important.[10] In later studies of multiple photoionization processes of Ne, various processes such as 2p, 2s, and 1s subshell electrons ionization can be clearly identified in the electron energy spectra as a function of the photon energy ranging from 100 eV to 2 keV and the spectra can be well reproduced by random-phase-approximation-with-exchange model which includes multielectron correlation of 2s subshell electrons.[11]

Compared to the energy spectra, differential cross sections such as photoelectron angular distribution contain more detailed information of the atomic system. For different electronic states and strength of electron correlations, the photoelectron angular distributions usually present profiles of different β asymmetry parameters[12] around the polarization direction, which can provide sensitive information on the electronic states which review the importance of electron correlation. The angular distribution β asymmetry parameters of helium satellites (up to 8) were firstly studied by Heimann *et al.*[13] It is found that, for excited electronic states, the β asymmetry parameter decreases as a function of the principal quantum number n, which is in good agreement with the dipole approximation. In a later work, it is found that the photoelectron angular distribution is independent of the photon energy

[†]These authors contributed equally to this work.
[‡]Corresponding author. E-mail: dingjj@lzu.edu.cn
[§]Corresponding author. E-mail: zhangshf@impcas.ac.cn

© 2023 Chinese Physical Society and IOP Publishing Ltd

in studies of satellite lines of Ar, which confirm the validity of angular-momentum transfer theory.[14] Adam *et al.*[15] measured the photoelectron satellites in the region of 3s Cooper minimum of Ar, and found that their photoelectron angular distributions are strongly dependent on the total angular momentum of the final ionic state.

In these early studies, the angular distributions of photoelectrons are obtained by electron spectrometers.[16] Cautious calibrations of the target and photon flux are necessary since only a particular direction of the emitted photoelectron can be monitored once a time with these spectrometers. Nowadays, the advent of the so-called reaction microscope has granted a 4π solid angle acceptance feasibility of detection efficiency. Such an accomplishment allows the accurate angular distribution measurement free of those beam calibrations.

In this work, photoelectron angular distributions of He and Ne are studied in single ionization via ultrashort XUV pulses by a reaction microscope. For XUV photon energy ranging from 22.1 eV to 43.7 eV, the β asymmetry parameters are systematically studied with high accuracy and comparisons with different theoretical results are discussed.

2. Experimental setup

The experiment was performed at the Institute of Modern Physics in which a dedicated reaction microscope has been built up in accordance with the XUV laser for ultrafast quantum dynamic studies.[17–19] For this particular study, the near-infrared pulses (3 kHz, 790 nm, 25 fs) are generated from the Ti:sapphire amplifier system and a peak intensity up to 10^{14} W/cm^2 can be achieved. The near-infrared laser is furtherly focused into a 5-cm-long, 150-μm-diameter waveguide,[20] in which the low pressure argon gas is fed in as the medium to generate XUV photons via the high harmonic generation (HHG) method.[21] The gas pressure inside the waveguide (around 50 Torr, 1 Torr = 133.3 Pa) is optimized to meet the phase matching condition according to the laser intensity, the pulse duration and the required harmonic orders. The XUV photons generated in the fiber are then focused on the supersonic gas target of the reaction microscope by a pair of toroidal mirrors. Detailed information of the reaction microscope can be found in previous report.[17–19,22]

Briefly, our gas target (He or Ne) is prepared via the supersonic expansion in a 30-μm nozzle under the pressure of 6 bar (1 bar = 10^5 Pa), which is picked up by two skimmers with 0.3-mm apertures, and the local density is estimated to be about 10^{10} atoms·cm^{-3} at the interaction area where the photon beam line across. After the absorption of one XUV photon, the target atom fragments into the recoil and the electrons. These charged particles are projected to different detectors by the hybrid of homogenous electric field (2.5 V/cm) and constant magnetic field (10 Gs, 1 Gs = 10^{-4} T). A voltage divider using a resistor chain ($R = 1$ MΩ, with 0.1% tolerance) is employed to maintain the uniform electric field in the acceleration region. The lengths of the acceleration region and drift region are 110 mm and 220 mm (1:2), respectively, satisfying the Wiley–McLaren time focusing condition. The constant magnetic field is applied in to confine the energetic electrons. Thus, a 4π acceptance solid angle can be achieved for electrons with kinetic energies up to 27 eV. The ions and electrons were detected in coincidence with the photon pulse given by the laser beam monitor. The information about the position and flight time of ions and electrons is obtained from which their momentum information can be extracted. In the following discussion, the coordinate system is defined as the following. The spectrometer arm is defined as x axis, and the polarization direction of the XUV photons (also is the gas jet direction) is denoted as y direction, meanwhile the photon propagation direction marks the z direction.

3. Results and discussion

In our experiment, the cut-off of the XUV spectra is at 46 eV which allows the single ionization of He and Ne, however other reaction channels such as ionization plus excitations and so on are prohibited due to the energy conservation. Figure 1(a) shows the kinetic energy distribution of photoelectrons generated from the ionization of He. The discrete structures of the photoelectron energy spectrum reflect the ionization resulting from different orders of harmonic. From these peaks, we can deduce the photon energies of each order of the high harmonic spectrum with high accuracy as 25.3±0.21 eV, 28.4±0.23 eV, 31.5±0.24 eV, 34.7±0.23 eV, 37.8±0.26 eV, and 40.8±0.33 eV, respectively. The yields of the photoelectrons show a monotonously decreasing tendency. Note that the yield is determined by two factors, the flux of harmonic orders and the total photoionization cross section. In the target of He, the latter one plays a dominant role, which decreases exponentially as a function of the photon energy.[23] As a comparison, the energy spectrum of the 2p photoelectrons of Ne is depicted in Fig. 1(b), where the incident photon energies of 22.1±0.23 eV, 25.2±0.23 eV, 28.3±0.22 eV, 31.5±0.21 eV, 34.5±0.21 eV, 37.6±0.22 eV, 40.7±0.35 eV, and 43.7±0.38 eV are obtained. A difference of about 3 eV in average can be seen in peaks of photoelectron from He and Ne, indicates the energy difference of first ionization potentials between them (24.58 eV and 21.6 eV). It can be seen from the spectra that, different from the ionization of He in Fig. 1(a), the photoionization yields for Ne present an increasing trend as a function of photon energy and then decrease. This is also due to the convolution of the total photoionization cross-sections of Ne, which increase at first and then decrease starting from the photon energy of 34 eV caused by the d wave moving to the initial wave functions,[23] and the flux of harmonic orders, which present an up and down trend with the maximum locating at about 38 eV.

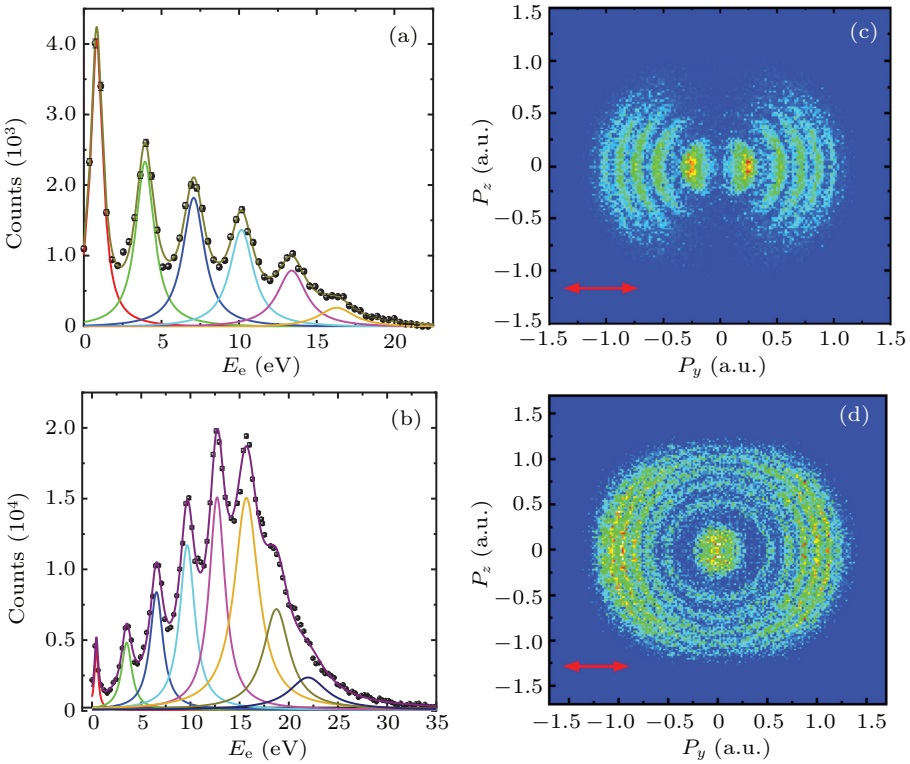


Fig. 1. Photoionization of He and Ne by different energy photons (different harmonics): (a) and (b) photoelectron spectra of He and Ne atoms, respectively, (c) and (b) photoelectron momentum distribution of He and Ne, respectively, in the plane formed by the light polarization (y, as indicated by the red double arrow) and the light propagation direction (z), for events with the momentum $|P_x| < 0.1$ a.u.

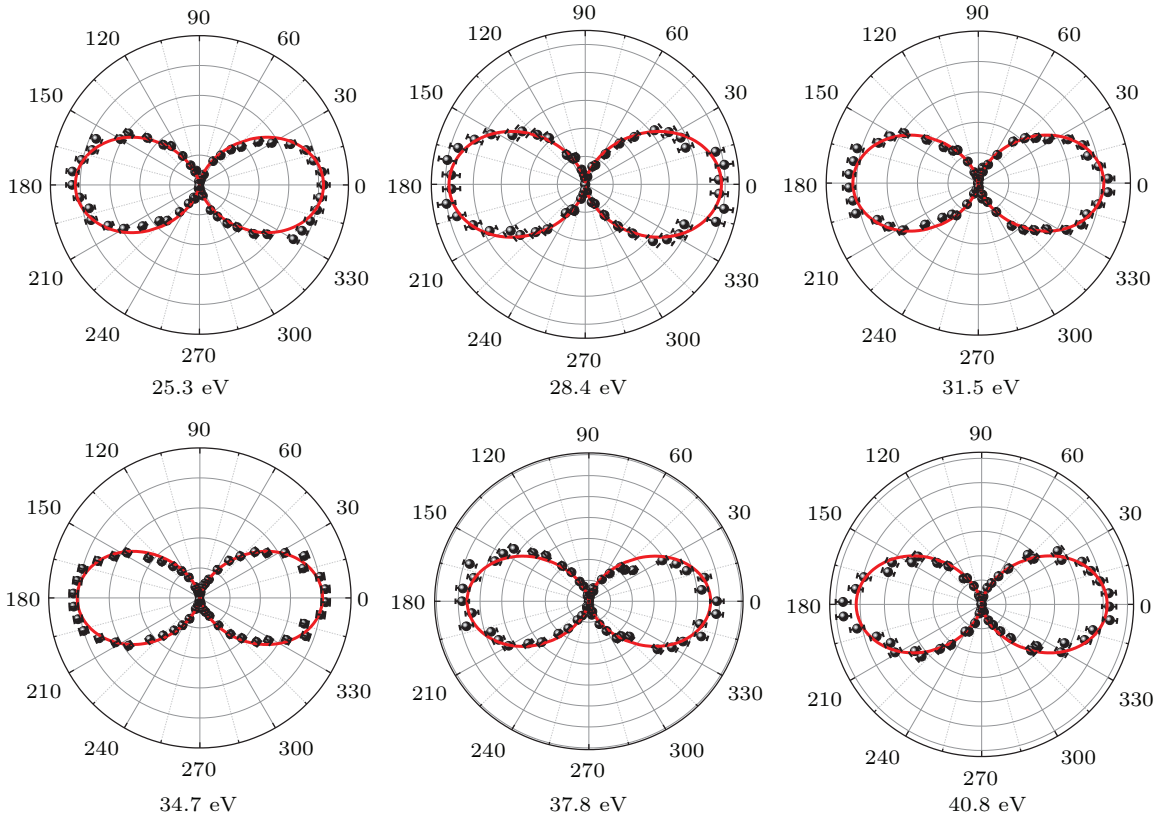


Fig. 2. The yield of photoelectrons from 1s shell of He atoms as a function of the angle between electron momentum and the polarization of incident XUV photon at different energies. Solid red lines are the fitting results of Eq. (1).

Figures 1(c) and 1(d) display the fully differential cross sections of photoelectrons from He and Ne ionization respectively, in the plane defined by the polarization direction (y-axis) and photon propagation direction (z axis). The red arrow represents the polarization axis of XUV photon. The condition of $|P_x| < 0.1$ a.u. is imposed in order to obtain clear angular

distribution in the P_y–P_z plane. For the same reason of discrete peaks in Figs. 1(a) and 1(b), the concentric rings observed in Figs. 1(c) and 1(d) are corresponding to the photoelectrons from He and Ne atoms after interaction with XUV photons in different energies. The outermost ring given in Fig. 1(c) arises from the ionization of He $1s^2$ electron by 40.8-eV XUV photon. Similarly, the outermost ring in Fig. 1(d) is caused by the ionization of Ne 2p electron with the incident photon energy of 43.7 eV. In both cases, clear dipole patterns can be observed from the photoelectron momentum distributions both for He $1s^2$ and Ne $2p^6$ electrons.

By measuring the full momentum components of each electron in different concentric rings in the slice, we obtain the distributions of angle between outgoing electron momentum and the polarization direction of XUV photons experimentally. Figure 2 exhibits the angular distributions of He 1s photoelectron with the photon energy range of 25.3 eV–40.8 eV. The black dots with error bars stand for the experimental results. It is clearly observed that the angular distributions of He atoms do not change significantly in the whole energy range.

Figure 3 shows 2p shell photoelectron angular distributions of Ne atoms measured with the photon energy ranging from 22.1 eV to 43.7 eV. For the XUV photons with the energy of 22.1 eV, the outgoing electrons tend to be emitted in the direction perpendicular to the laser polarization. Increasing the photon energy to the range between 25.2 eV and 28.3 eV, the photoelectron angular distribution becomes isotropic gradually (see Figs. 3(b) and 3(c)). With further increase in the photon energy (above 28.3 eV), the electrons tend to be ejected along the XUV polarization direction (Figs. 3(d) and 3(h)).

Theoretically, the photoelectron angular distribution in the dipole approximation can be described by[12]

$$\frac{\mathrm{d}\sigma(E)}{\mathrm{d}\Omega} = \frac{\sigma(E)}{4\pi}(1+\beta(E)\mathrm{P}_2(\cos\theta)), \tag{1}$$

where $\mathrm{d}\sigma(E)/\mathrm{d}\Omega$ is the fully differential cross section of the photoionization, E is the photon energy, $\sigma(E)$ is the photoionization total cross-section, θ is the electron emission angle with respect to the XUV polarization direction, P_2 is the Legendre polynomial with $\mathrm{P}_2(\cos\theta) = \frac{1}{2}(3\cos^2\theta - 1)$, and β is the asymmetry parameter, which is from -1 to 2. The character of electron angular distribution can be described by β. When β is positive, it indicates that electrons tend to be emitted along the direction of light polarization. If β is negative, electrons are more likely to be emitted perpendicular to light polarization direction, as β is 0, electrons tend to be emitted isotropically. By fitting angular distributions of photoelectrons at different energies with Eq. (1), shown as the solid red line in Figs. 2 and 3, the β asymmetry parameters are obtained. As mentioned already, the merit of reaction microscope can collect the charged particles with 4π solid angle simultaneously, which reduce the systematic uncertainty essentially because no calibration on target density is needed. Consequently, the sources of error are only statistics and noise, and the present experimental data are more precise compared with the results of Codling[24] and Dehmer.[25] All the datasets in this paper including photoelectron angular distributions and β asymmetry parameters for single ionization of He and Ne have been compiled in the supplementary materials (SM).

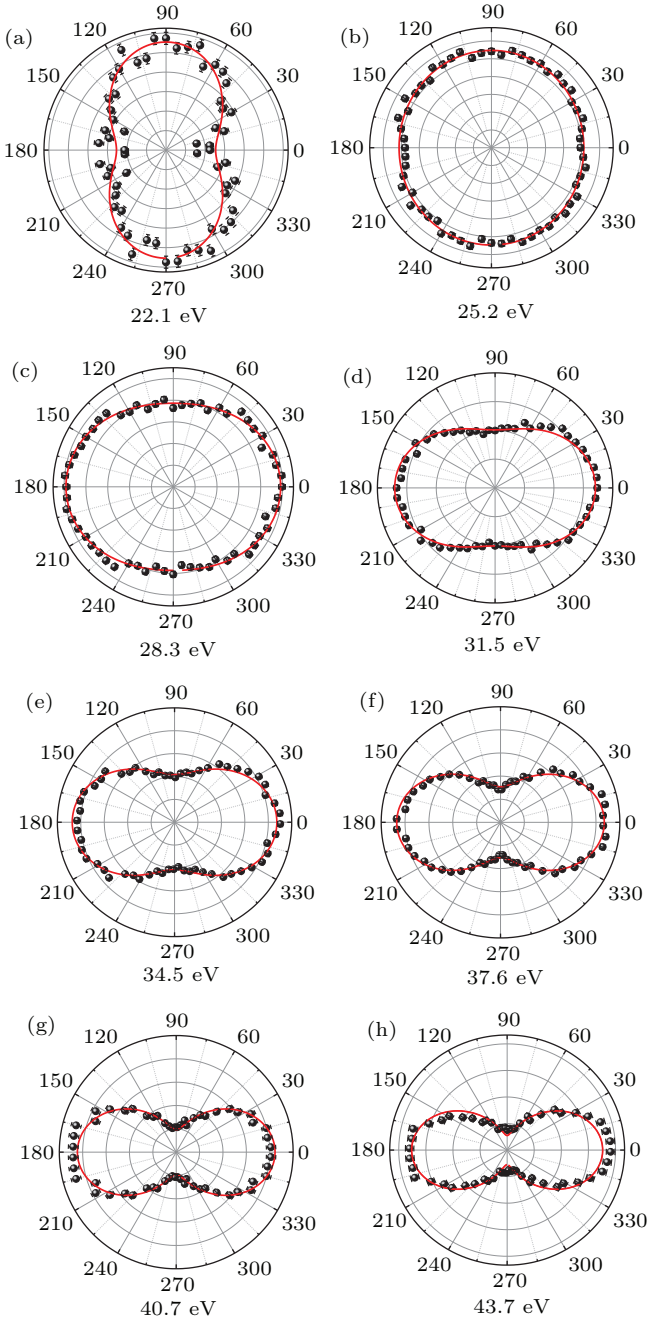


Fig. 3. The photoelectron yield of 2p shell of Ne as a function of emission angle with photon energy range from 22.1 eV to 43.7 eV. Black dots with the error bars represent the experimental data and red solid lines show the fitting by Eq. (1).

Table 1 shows the β asymmetry parameters of the angular distribution of He $1s^2$ electron for different incident photon energies. It is found that the β asymmetry parameters are roughly equal to 2 for different energy photons. The β asymmetry parameter of He is insensitive to the photon energy since

(i) there is only one transition of s → p for single ionization of He and no competing channels exist which can cause interferences; (ii) higher order contributions such as the relativistic effects and so on are negligible in the ground 1s state of He. This observation is in good accordance with the reported theory result,[26] and we can safely conclude that results obtained from our reaction microscope measurements are reliable.

Table 1. Angular asymmetry parameters β of 1s electrons of He atoms for different photon energies.

Photon energy (eV)	β_{1s}
25.3±0.21	2.03±0.07
28.4±0.23	1.97±0.08
31.5±0.24	2.05±0.08
34.7±0.23	2.07±0.05
37.8±0.26	2.00±0.08
40.8±0.33	1.97±0.10

Table 2. Angular asymmetry parameters β of 2p electrons of Ne atoms for different photon energies.

Photon energy (eV)	β_{2p}	Ref.
22.1±0.23	–0.440±0.03	present work
25.2±0.23	–0.045±0.02	
28.3±0.22	0.173±0.02	
31.5±0.21	0.393±0.01	
34.5±0.21	0.560 ±0.02	
37.6±0.22	0.727±0.02	
40.7±0.35	0.830±0.04	
43.7±0.38	0.920±0.06	
22.8	–0.561±0.15	Codling *et al.*[24]
23.7	–0.429±0.10	
24.7	–0.268±0.10	
26.6	0.038±0.07	
28.4	0.233±0.07	
32.6	0.619±0.20	
36.5	0.864±0.20	
40.6	1.005±0.15	
44.7	0.947±0.17	
54.7	1.079±0.15	
61.4	1.268±0.17	
64.4	1.262±0.19	
74.4	1.040±0.20	
84.4	1.209±0.25	
102.0	1.330±0.15	
26.9	0.116±0.05	Dehmer *et al.*[25]
40.8	0.812±0.05	
48.3	1.010±0.05	

As for Ne $2p^6$ photoionization, the obtained angular β asymmetry parameters are shown in Table 2, which change substantially as increase of incident photon energy. In the dipole approximation, the initial state of atom A is defined by the orbital angular momentum, spin angular momentum, total angular momentum, and parity quantum numbers $\boldsymbol{L}_\mathrm{i}$, $\boldsymbol{S}_\mathrm{i}$, $\boldsymbol{J}_\mathrm{i}$, and π_i. The incident photon γ can be considered as imparting an angular momentum $\boldsymbol{j}_\gamma = 1$ and parity $\pi_\gamma = -1$ to the atom. If the final state of the ion A^+ is specified by $\boldsymbol{L}_\mathrm{f}$, $\boldsymbol{S}_\mathrm{f}$, $\boldsymbol{J}_\mathrm{f}$, and π_f, and the emitted photoelectron by l, s, j, $\pi_\mathrm{e} = (-1)^l$, the photoionization processes by linearly polarized light in the nonrelativistic case of *LS* coupling have to obey two restriction rules:

$$|\boldsymbol{J}_\mathrm{i} - 1| \le \boldsymbol{J}_\mathrm{f} \le \boldsymbol{J}_\mathrm{i} + 1. \tag{2}$$

Besides, the constraints of parity conservation must also be considered:

$$\pi_\mathrm{i} \times \pi_\gamma = \pi_\mathrm{f} \times \pi_\mathrm{e}, \tag{3}$$

which in the dipole approximation reduces to $\pi_0 \pi_\mathrm{c} = -1$. Therefore, for the Ne ionization process,

$$\begin{aligned} &\mathrm{Ne}\left(2\mathrm{p}^6\ {}^1\mathrm{S}_0, \pi_0 = +1\right) + \gamma\left(j_\gamma = 1, \pi_\gamma = -1\right) \\ &\rightarrow \mathrm{Ne}^+\left(2\mathrm{p}^5\ {}^2\mathrm{P}_{3/2,1/2}, \pi_\mathrm{c} = -1\right) + e(l, \pi_\mathrm{e}) \end{aligned} \tag{4}$$

according to the parity and angular momentum conservation, the allowed orbital angular momentum l of outgoing electrons are determined to be 0 and 2. According to Refs. [12,27–29], the energy-dependence of β parameter appears as a result of interference of the amplitudes and phases for two transitions: p → s and p → d.

Figure 4 illustrates the asymmetry parameters β_{2p} of Ne atoms as a function of incident photon energies from 22.1 eV to 43.7 eV. The solid circles, open triangle, and circles are the experimental data of our work, Codling *et al.*,[24] and Dehmer *et al.*,[25] respectively. The dash black line and blue solid line are the results from random-phase-approximation (RPA),[30] and Hartree–Fock (HF) calculation of the β asymmetry parameters for 2p photoionization of Ne, respectively. Orange dash line and red dot line are Dirac–Fock (DF) calculations for the $P_{1/2}$ and $P_{3/2}$ subshells.[31] Essentially, all the above theoretical models deal in different steps of approximations with two effects: (i) the influence of the Coulomb interaction effect among the electrons (electron interaction and configuration interaction) which results in electron correlation effects and (ii) the influence of relativistic effects as for example the spin–orbit interaction. Relativistic effects are taken into account in D-F calculation, while the electron correlation effect is omitted. RPA calculation contains significant aspects of electron–electron correlation in initial and final state wave functions of the photoionization process, but does not take relativistic effect into account. Our HF calculation is a single active particle model, that is, the active electrons are described using a single-particle orbital wavefunction. The active electron feels the presence of the other electrons indirectly through an effective potential. This method, hence, neglects both relativistic effects and the electron correlation effects. The observed β asymmetry parameter for 2p photoelectron of Ne displays a monotonic variation with photon energy, and its curve shape is excellently reconstructed by the RPA calculation, while DF theory is different from the experimental data, as shown in Fig. 4. This indicates the influence of relativistic effect is small in 2p photoionization of Ne, but electron correlation is important in this process. It should be noted that, when the photon energy is below 23.5 eV (near the first ionization threshold), the results obtained by HF calculation and RPA theory are very

similar and in good agreement with the experimental data. As the energy of the incident photon increases, the RPA theory is more consistent with the experimental value than the HF theory. That means the influence of electron correlation effect on the angular distribution for Ne $2p^6$ ionization is small, when the photon energy is below the first ionization threshold. With the incident photon energy increasing, the electrons correlation effect becomes significant for photoelectron angular distribution in photoionization process.

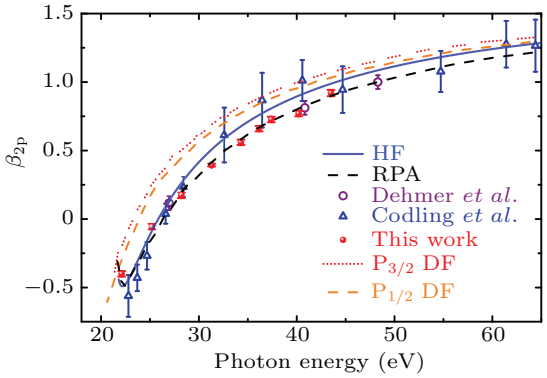


Fig. 4. Angular distribution asymmetry parameter β for 2p photoelectrons of Ne with different photon energies. The red solid circles, open triangles, and circles are results of experiments. The solid line and the dash lines are calculation results.

4. Summary

Combination of the tabletop XUV source with the well-developed reaction microscope offers powerful tools for investigating the electron dynamical processes. We have measured photoelectron momentum distributions: single photon ionization of He and Ne atoms induced by linearly polarized XUV photons whose energy ranging from 22.1 eV to 43.7 eV. Photoelectron angular distributions of He 1s ionization are found to be energy-independent, and the asymmetry parameters β_{1s} are measured to be 2, proving our experiment system reliability. For 2p ionization of Ne, with the increase of photon energy, the angular distributions of photoelectrons flip from perpendicular to the polarization direction to along the polarization direction. By comparing the RPA, HF, and DF calculations with our experimental results of Ne 2p ionization, it is found that, the electron correlation effect is small when the photon energy is lower than the first ionization threshold, and becomes increasingly important as the incident photon energy increases, while the relativistic effect is small in whole incident photon energy range. These experimental results gain insight into the theoretical models of electron interactions and promote studies of relevant fundamental processes by providing the benchmark data for testing different theoretical models.

Data availability statement

The data that support the findings of this study are openly available in Science Data Bank at the following site: https://doi.org/10.57760/sciencedb.j00113.00073.

Acknowledgements

The authors are grateful to Dr. Najjari B for providing us with the HF calculation. Project supported by the National Natural Science Foundation of China (Grant Nos. 11905089 and U1932133) and the National Key Research and Development Program of China (Grant No. 2017YFA0402300).

References

[1] Feldhaus J, Krikunova M, Meyer M, Möller T, Moshammer R, Rudenko A, Tschentscher T and Ullrich J 2013 *J. Phys. B: At. Mol. Opt. Phys.* **46** 164002
[2] Goulielmakis E, Loh Z H, Wirth A, Santra R, Rohringer N, Yakovlev V S, Zherebtsov S, Pfeifer T, Azzeer A M and Kling M F 2010 *Nature* **466** 739
[3] Jiang Y H, Rudenko A, Kurka M, Kühnel K U, Foucar L, Ergler T, Lüdemann S, Zrost K, Ferger T and Fischer D 2009 *J. Phys. B: At. Mol. Opt. Phys.* **42** 134012
[4] Rudenko A, Foucar L, Kurka M, Ergler T, Kühnel K U, Jiang Y H, Voitkiv A, Najjari B, Kheifets A, Lüdemann S, Havermeier T, Smolarski M, Schössler S, Cole K, Schöffler M, Dörner R, Düsterer S, Li W, Keitel B, Treusch R, Gensch M, Schröter C D, Moshammer R and Ullrich J 2008 *Phys. Rev. Lett.* **101** 073003
[5] Chen Z, Liang Y, Madison D H and Lin C D 2011 *Phys. Rev. A* **84** 023414
[6] Saenz A and Lambropoulos P 1999 *J. Phys. B: At. Mol. Opt. Phys.* **32** 5629
[7] Hart H W V D and Bingham P 2005 *J. Phys. B: At. Mol. Phys.* **38** 207
[8] Svensson S, Eriksson B, Mårtensson N, Wendin G and Gelius U 1988 *J. Electron Spectrosc. Relat. Phenom.* **47** 327
[9] Kikas A, Osborne S J, Ausmees A, Svensson S, Sairanen O P and Aksela S 1996 *J. Electron Spectrosc. Relat. Phenom.* **77** 241
[10] Carlson T A 1967 *Phys. Rev.* **156** 142
[11] Wuilleumier F and Krause M O 1974 *Phys. Rev. A* **10** 242
[12] Manson S T and Starace A F 1982 *Rev. Mod. Phys.* **54** 389
[13] Heimann P A, Becker U, Kerkhoff H G, Langer B, Szostak D, Wehlitz R, Lindle D W, Ferrett T A and Shirley D A 1986 *Phys. Rev. A* **34** 3782
[14] Langer B, Viefhaus J, Hemmers O, Menzel A, Wehlitz R and Becker U 1995 *Phys. Rev. A* **51** R882
[15] Adam M Y, Morin P and Wendin G 1985 *Phys. Rev. A* **31** 1426
[16] Roy D and Tremblay D 1990 *Rep. Prog. Phys.* **53** 1621
[17] Hai B, Zhang S F, Zhang M, Najjari B, Dong D P, Lei J T, Zhao D M and Ma X 2020 *Phys. Rev. A* **101** 052706
[18] Zhang M, Hai B, Zhao D M, Lei J T, Dong D P, Zhang S F and Ma X W 2020 *Chin. Phys. B* **29** 63302
[19] Ullrich J, Moshammer R, Dorn A, Drner R, Schmidt L P H and Schmidt-B cking H 2003 *Rep. Prog. Phys.* **66** 1463
[20] McKinnie I and Kapteyn H 2010 *Nat. Photon.* **4** 149
[21] Corkum P B and Krausz F 2007 *Nat. Phys.* **3** 381
[22] Dörner R, Mergel V, Jagutzki O, Spielberger L, Ullrich J, Moshammer R and Schmidt-Böcking H 2000 *Phys. Rep.* **330** 95
[23] Samson J A R and Stolte W C 2002 *J. Electron Spectrosc. Relat. Phenom.* **123** 265
[24] Codling K, Houlgate R G, West J B and Woodruff P R 1976 *J. Phys. B: At. Mol. Phys.* **9** L83
[25] Dehmer J L, Chupka W A, Berkowitz J and Jivery W T 1975 *Phys. Rev. A* **12** 1966
[26] Krause M O, Whitfield S B, Caldwell C D, Wu J Z, van der Meulen P, de Lange C A and Hansen R W C 1992 *J. Electron Spectrosc. Relat. Phenom.* **58** 79
[27] Dill D and Fano U 1972 *Phys. Rev. Lett.* **29** 1203
[28] Dill D 1973 *Phys. Rev. A* **7** 1976
[29] Fano U and Dill D 1972 *Phys. Rev. A* **6** 185
[30] Schmidt V 1986 *Z. Phys. D: At., Mol. Clusters* **2** 275
[31] Ong W and Manson S T 1980 *Phys. Rev. A* **21** 842